King Saud University

Arabian Journal of Chemistry

www.ksu.edu.sa
www.sciencedirect.com

Eco-friendly synthesis of *Cynomorium coccineum* extract for controlled production of copper nanoparticles for sorption of methylene blue dye

Nouha Sebeia [b], **Mahjoub Jabli** [a,b], **Adel Ghith** [b], **Tawfik A. Saleh** [c,*]

[a] *Department of Chemistry, College of Science Al-Zulfi, Majmaah University, Saudi Arabia*
[b] *Textile Materials and Process Research (LMPTEX), National School of Engineering of Monastir (ENIM), Monastir 5000, Tunisia*
[c] *Chemistry Department, King Fahd University of Petroleum & Minerals, Dhahran 31261, Saudi Arabia*

Abstract   A biological extract of *Cynomorium coccineum* was used for the synthesis of copper nanoparticles using copper sulphate as a starting matter. Fourier transform infrared spectroscopy (FT-IR) showed the presence of the functional groups characteristics of biological extract, i.e., triterpenes, phenolics, flavonoids, and other reducing agents. SEM analysis showed that the surface of the particles were clusters and rough. The Elemental analysis by energy-dispersive X-ray (EDX) proved the purity of the particles, showing the presence of elemental copper oxide which was surrounded with some elements of the plant. X-ray diffraction (XRD) pattern confirmed that the crystalline nature of the particles was affected by temperature. The average crystallite size was calculated to be about 14.2 nm. The total weight loss registered within the thermogravimetric (TG) analysis was 52.8%, suggesting that about 47.2% of the metallic copper is present in the prepared copper nanoparticles which supported the data reported within EDX analysis. The adsorption characteristics of the nanoadsorbents were examined using methylene blue as adsorbate and the bio-sorption capacity reached 64 mg/g at room temperature. The values of B and b_t, calculated from Temkin equation, increased with the increase in temperature (295–328 K), indicating endothermic adsorption and strong dye-nanoadsorbent interaction. The mean free energy ($E = 100$–129.1 kJ/mol), calculated from Dubinin-Radushkevich indicated that the chemisorption

* Corresponding author.
  E-mail address: tawfik@kfupm.edu.sa (T.A. Saleh).
  URL: http://faculty.kfupm.edu.sa/CHEM/tawfik/publications.html (T.A. Saleh).
Peer review under responsibility of King Saud University.

ELSEVIER   **Production and hosting by Elsevier**

is the process involved for the adsorption of methylene blue. In summary, the results obtained in this study deliver the design and the synthesis of new materials for removing pollutants.

1. Introduction

Nanomaterials have been widely used in many fields since their unique properties compared with common materials (Hou et al., 2019). Recently, natural products have gained more attention due to the global development of maintaining good health and reducing the risk of disease (Suwalsky et al., 2008). In this framework, many materials were studied as sources of bio-products (Xu et al., 2019; Shi et al., 2019). The important characteristics of such plant extract, including phenols, flavonoids, and other bio-products, were proved to be, in particular, responsible for the reduction of metal salts into nanoparticles (Aromal et al., 2012). These nanoparticles were recognized for their large surface area, small size, and other physicochemical parameters which make them useful for many applications such as dye removal (Saleh and Al-Absi, 2017), antioxidant, diabetic, anti-inflammatory (Govindasamy et al., 2018), antibacterial activities (Singh et al., 2013; Sun et al., 2019), energy storage systems and other applications (Sheikholeslami and Mahian, 2019; Saleh, 2015a,b).

The nanoparticles were, principally, used in the degradation of hazardous and toxic pollutants (Li et al., 2019; Saleh, 2016,2018). The literature reported the successful synthesis of copper nanoparticles through a green approach where *Capparious zeylanica* (Saranyaadevi et al., 2014); *Ocimum sanctum* (Patel et al., 2016); *Vitis vinifera* (Angrasan and Subbaiya, 2014); *Azadirachta indica* (Nagar and Devra, 2018), as well as various other plant extracts, were used as reducing and capping agents. The characteristics of these synthesized nanoparticles depended on the source of the plant extract (Shankar et al., 2004; Mukunthan and Balaji, 2012). The consideration of these biological sources for the synthesis of nanoparticles is more beneficial than the chemical methods as these sources are abundantly available, cost-effective and conveniently applicable.

Cynomorium coccineum L. is a non-photosynthetic plant, spread over the south of Spain to the southern Italian coast, Sardinia, Sicily, Malta and from the West African coast to North African coast (The Canary Islands to Tunisia) (Abd El-Rahman et al., 1999; Dharmananda, 2011; Duke et al., 2008.). It is a blackish red leafless root parasitic plan (Heestra et al., 1990). It is known as traditional medicine and it is reported to enclose a hypotensive effect (Ikram et al., 1978). To our best knowledge, *Cynomorium coccineum* was not investigated as a biological extract for the synthesis of metal nanoparticles. Our previous work was focalized on the extraction of dye molecules from *Cynomorium coccineum*. The prepared aqueous colored extract was characterized for Total Flavonoids (TFC), Total Phenols (TPC) contents and the antioxidant activity (Jabli, 2017) and good results were registered. Herein, we explore for the first time the biological molecules of *Cynomorium coccineum* extract for the green synthesis of copper nanoparticles as nanoadsorbents. To understand the molecular-level interactions, the prepared nanoparticles were analyzed using Fourier Transform Infrared Spectroscopy, Scanning Electron Microscopy, Energy-dispersive X-ray spectroscopy, X-ray Diffraction, and thermogravimetric analysis. The prepared particles were, then, used as nanoadsorbents of methylene blue from aqueous suspension under several experimental conditions using batch mode. The sorption data were correlated to the theoretical kinetic (pseudo-first order, pseudo-second-order, Elovich, and intra-particular diffusion) and common isotherms equations (Langmuir, Freundlich, Temkin, and Dubinin-Radushkevich). The corresponding parameters were computed to better understand the adsorption mechanism.

2. Experimental

2.1. Chemical and reagents

All used chemicals and reagents: copper sulfate (precursor salt), ethanol, acetone, etc. were of analytical grade. In this study, methylene blue, supplied from Sigma Aldrich, was used as adsorbate and representative of cationic dyes. Its molecular weight was 319.85 g mol^{-1}. Their physico-chemical characteristics were summarized in Table 1. Distilled water was used to prepare aqueous solutions and for finishing experiments (washing and rinsing). The pH was adjusted using 0.1 M HCl or 0.1 M NaOH solutions.
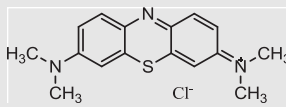
### 2.2. Preparation of Cynomorium coccineum aqueous extract

The fractions of *Cynomorium coccineum* were collected during the month of March 2019 from Skanes region area (latitude: 35°75′, longitude: 10°82′), Governorate of Monastir, Tunisia. The collected fractions were thoroughly washed and shade dried for a weak and ground to fine powdered using an electrical mixer. Grinded dried *Cynomorium coccineum* fractions (10 g) were heated in a flask containing 150 mL distilled water for 90 min at 70 °C. After which, it was cooled to room temperature and then filtrated with a filter paper.

2.3. Bio-synthesis of copper nanoparticles using Cynomorium coccineum extract

The freshly prepared *Cynomorium coccineum* extract (100 mL) was added to 100 mL of 1 M copper sulfate solution. The mixture was constantly stirred at 70 °C for 2 h. The color change of the solution from blue to dark green indicated the formation of the copper nanoparticles (Fig. 1). Afterward, it was cooled to room temperature and then filtrated using a filter paper. Finally, the synthesized nanoparticles were subjected to drying at 100 °C for a period of 12 h.

Table 1 Physico-chemical characteristics of methylene blue dye.

Name	Chemical structure	λ (nm) in water	Molecular weight (g/mol)	Empirical Formula
Methylene blue		664	319.85	$C_{16}H_{18}ClN_3S$
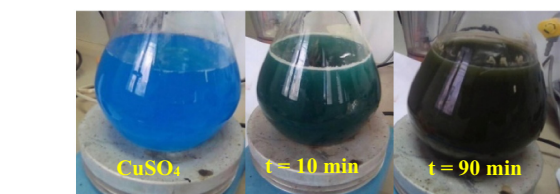
Fig. 1 Photographs showing the extraction of dye from *Cynomorium coccineum* and the change in color during the synthesis of the copper nanoparticles.

2.4. Characterization techniques

Fourier Transform Infrared Spectroscopy was used to identify the functional groups characteristics of the bio-molecules present in *Cynomorium coccineum* extract. The FT-IR spectra were recorded on a Perkin Elmer model in the 4000–400 cm^{-1} region using KBr pellet method. The morphological features of the samples were evaluated by a SEM Hitachi S-2360N. Samples were coated with Au by a vacuum sputter-coater with 20 kV accelerating voltage. EDX measurements were taken on a Philips FEI Quanta 200 for semi-quantitative analysis of elements. X-ray powder diffractograms were obtained at room temperature on a PANalytical X'Pert PRO MPD apparatus. Thermal analysis (TGA) experiments were performed in the air flow at a heating rate of 10°/min in a Pt crucible with NETZSCH STA 449F3 equipment.

2.5. Bio-sorption batch procedure

The batch sorption experiments were carried out in Erlenmeyer flasks containing 0.025 g of the prepared copper nanoparticles and a dye volume of 20 mL. The mixture was agitated at 125 rpm for different periods of time after the equilibrium was reached. The effect of initial pH value on the adsorption of methylene blue was studied in the range 3–10. The nanoadsorbent dosage was investigated in the range 0.0125–0.1 g. The effect of the change of temperature was examined at the range 22–55 °C. The absorbance evolution of the colored solutions was monitored through UV–Vis spectrophotometer at a wavelength of 664 nm. The adsorbed amount of methylene blue was calculated according to the following formula:

$$q\left(\frac{mg}{g}\right) = \frac{(c_0 - c_e)}{m} \times V \tag{1}$$

where c_0 and c_e are the initial and residual dye concentration. V is the volume of the used adsorbate during the adsorption experiments and m is the mass of the used adsorbent.

3. Results and discussion

3.1. Copper nanoparticles characterization

Fig. 2 showed the different functional groups characteristics of *Cynomorium coccineum* extract and the associated biological synthesized copper nanoparticles. In the spectrum of the *Cynomorium coccineum* extract, the bands at 3223, 2882–2801, 1593, and 1312–1195 cm^{-1} were attributed to the O—H stretching of alcohol and phenol, C—H stretching of the aliphatic group, C═C stretching of the aromatic ring, and C—O stretching of ester, respectively (Subbaiya et al., 2014; Tahir et al., 2015). The intense absorption band observed at 1014 cm^{-1} could be assigned to C—O—C stretching vibration (Tahir et al., 2015). The spectrum of the biosynthesized copper nanoparticles did not change much compared with the extract and it showed the main characteristic peaks with band shifting. In fact, the band observed for hydroxyl groups at 3223 cm^{-1} in the spectrum of the studied extract shifted to a lower value (3199 cm^{-1}) in the spectrum of the prepared nanoparticles. This shifting, at this position and the decrease in its intensity, might indicate that the copper ions interacted with OH groups. This trend suggested that the prepared particles were surrounded by different organic bio-molecules. Regarding the spectrum of methylene blue adsorbed onto the prepared nanoparticles, such a shift in the band characteristics proved the interaction between the dye molecules and the copper nanoparticles. Overall, the results obtained from the FT-IR spectra confirmed that the prepared nanoparticles are coated with bio-molecules that acted as both reducer and coating for copper nanoparticles against oxidation.

In fact, the formation mechanism of the copper nanoparticles could be explained by the fact that the bio-molecules (i.e. Flavonoids, phenolics, etc.) present in *Cynomorium coccineum* extract can act as ligation agents. The hydroxyl groups of the bio-molecules form complexing agents with the copper sulfate as precursor salts and therefore ligate with copper ions. This starts the nucleation process that goes into reverse micellization, which then causes the reduction of the nanoparticles. This system undergoes decomposition when the particles are dried at elevated temperatures leading to the easy release of the CuO nanoparticles from the copper-ellagate complex system (Yuvakkumar et al., 2014). According to literature, the major constituents of *cynomorium* plants have been identified to be
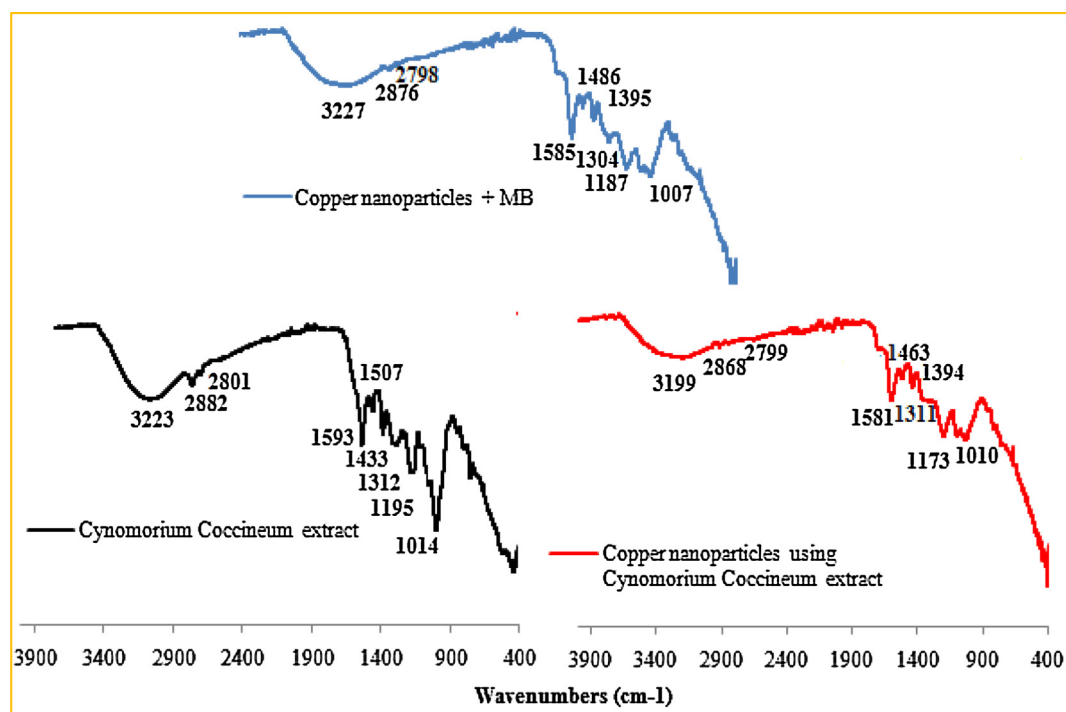
Fig. 2 FT-IR spectrum of *Cynomorium coccineum* extract and their associated biological copper nanoparticles before and after their interaction with methylene blue dye.

phenolic compounds, steroids, triterpenes, etc. (Hao-Cong et al., 2013). In Fig. 3, we propose the formation of copper nanoparticles using the biological *Cynomorium coccineum* extract.

Fig. 4a–b depicted the SEM photos of the prepared copper nanoparticles with higher magnifications. Data revealed that the studied samples were clustered with a rough surface. As, also, observed, the images indicated that the nanoparticles were both mono-dispersed and agglomerated with almost spherical morphologies. Such variation in particles size and shape distribution is related to the chemical composition of the *Cynomorium coccineum* extract.

Fig. 4c gave the EDX spectrum of the synthesized copper nanoparticles. The strong signal energy peaks for the copper atoms were observed at 1.0 and 8.0 keV, which correlated well with the previous studies carried out for the synthesis of copper nanoparticles (Cerchier et al., 2017; Ebrahimi et al., 2017). It was registered that approximately 54.1% weight of copper was present in the prepared nanoparticles. The remaining 45.9% were carbon and oxygen present in organic molecules that acted as capping molecules surrounding the nanoparticles. In fact, the presence of carbon (26.52%) and oxygen (19.38%) elements was due to the phytochemicals enclosed in *Cynomorium coccineum* extract (Valodkar et al., 2011). The absence of the impurities in the EDX profile is indicative of the purity of the biosynthesized CuO nanoparticles.

The XRD pattern of the prepared samples dried at either 60 °C or 100 °C is given in Fig. 5. The as-obtained copper nanoparticles dried at 60 °C show a broad pattern, which has been attributed to the highly amorphous and bio-capped

nanoparticles. However, after drying these copper nanoparticles at 100 °C for about 12 h in a vacuum oven, the bio-capping were partially removed. The peaks observed at $2\theta = 43.2°$, 49.5°, and 74° correspond to (1 1 1), (2 0 0) and (2 2 0) representing a face-centered cubic structure of copper (JCPDS No. 85–1326). The same trends were reported within the synthesis of copper nanoparticles using Terminalia arjuna bark extract (Yallappa et al., 2013) and using the aqueous extract of Calotropis procera L. latex (Harne et al., 2012). In fact, sintering processing is known to improve the crystallinity and the particle size.

The average crystallite size (expressed as D) of the prepared copper nanoparticles was calculated to be about 14.2 nm using Debye–Scherrer equation (Yallappa et al., 2013):

$$D = \frac{K\lambda}{\beta_{1/2}cos\theta} \tag{2}$$

where D is the crystallite size, K is the shape factor between 0.9 and 1.1, λ is the incident X-ray wavelength (Cu Kα radiation = 1.542 Å). $\beta_{1/2}$ is the full-width half maximum in radians of the prominent line and θ is the position of that line in the pattern.

Fig. 5b shows the TGA curve of the synthesized copper nanoparticles. The initial weight loss of 11% from room temperature to 110 °C corresponds to the adsorbed water molecules. The subsequent weight loss of 41.8% from 219 °C to 786 °C is attributed to the degradation of plant residue i.e., the bio-capping material present on the prepared nanoparticles (Kasthuri et al., 2009). The total weight loss registered within the thermogram was 52.8%, showing that about 47.2% of the metallic copper is present in the prepared copper
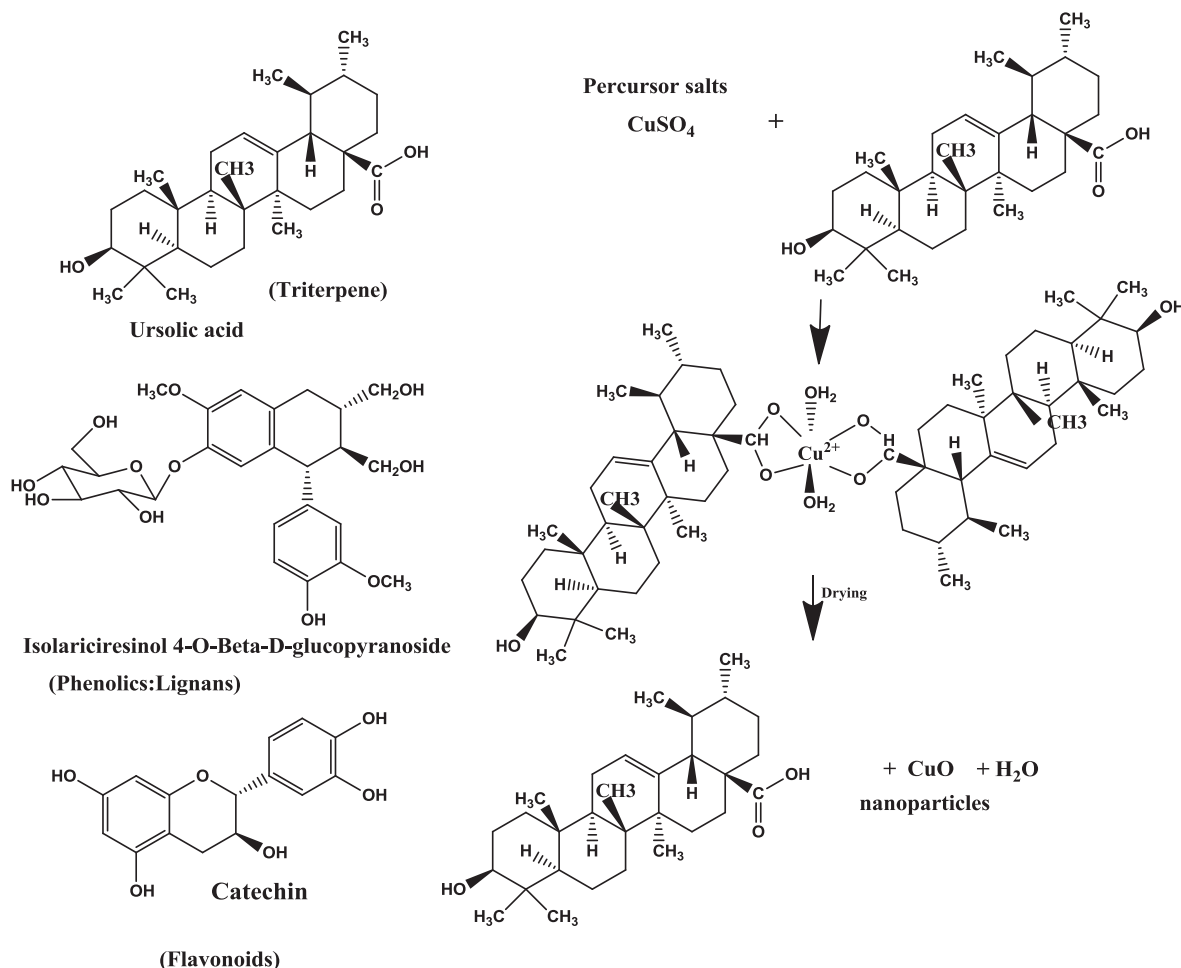
Fig. 3 Possible mechanism of the formation of copper nanoparticles using biological *Cynomorium coccineum* extract.

nanoparticles. This behavior supports the data reported within the EDX analysis.

3.2. Factors influencing the sorption capacities of methylene blue using the nano-adsorbents

The effect of the change of initial pH value on the bio-sorption of methylene blue in the presence of the prepared nano-adsorbents (Fig. 6a) exhibited that the adsorbed amount of dye increased with increasing pH in the range of 3–6. The maximum sorption amount was achieved at pH 6. The small adsorption capacity at lower pH could be explained by the fact that protons are available on the surface of the nanoparticles used as adsorbent which causes electrostatic repulsion between the cationic dye and the adsorbed H$^+$ ions. However, at higher pH values, the enhancement in dye sorption capacities could be explained by the occurrence of electrostatic forces of attraction between the positively charged dye cations and the negatively charged surface of the studied adsorbent.

Regarding the effect of the adsorbent dosage on the adsorption phenomenon, the adsorbent amount of methylene blue depended on the mass of the nanoadsorbent (Fig. 6b). The maximum adsorption amount was achieved using 0.025 g of the mass of the adsorbent. It reached 5.47 mg/g ($C_0 = 25$ mg/g, $t = 30$ min, T = 22 °C). However, it did not exceed 1.8 mg/g within a mass of 0.1 g of the adsorbent under the same experimental conditions. The high sorption amount of methylene blue adsorbed per unit mass of the studied nanoadsorbent registered at low adsorbent dosages (0.0125–0.025) could be explained by the fact that the adsorption sites remained unsaturated during the adsorption reaction (Wei et al., 2005). This agreed with the results obtained in our previous work dealing with the bio-sorption of methylene blue using populus tremula, pergularia tomentosa, and nerium oleander as bio-sorbents (Sebeia et al., 2019). Similar quite a tendency has been, also, reported using other sorbents (Barka et al., 2011; Bulut and Aydın, 2006; Osasona et al., 2013).

The sorption equilibrium of methylene blue was achieved after only 30 min of time contact (Fig. 5c). The sorption rate was fast within the first 10 min and it became slower at the range 30–60 min. This could be explained by the availability of the adsorption sites in the first period of time contact. The observed rapid sorption rates suggest, also, the efficiency of the prepared particles as nano-adsorbents of organic dyes.
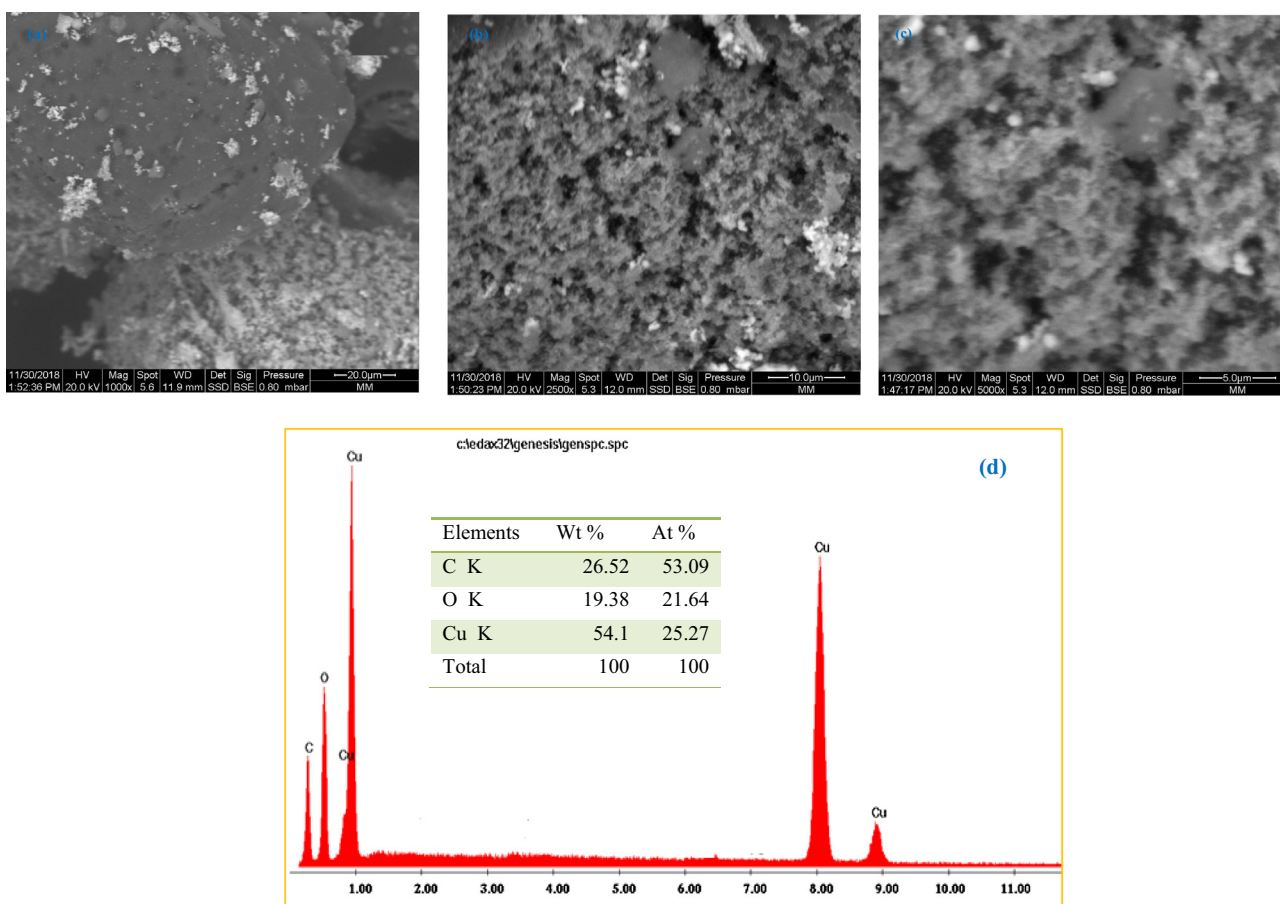
Elements	Wt %	At %
C K	26.52	53.09
O K	19.38	21.64
Cu K	54.1	25.27
Total	100	100

Fig. 4 SEM images of copper nanoparticles synthesized using *Cynomorium coccineum* extract with different magnifications: (a) 1000×, (b) 2500×, (c) 5000×, and (d) the elemental analysis determined by EDX.

This adsorbed amount of dye molecules per unit mass of adsorbent increased with the increase in dye concentration (Fig. 6d). In fact, in the case of the low initial concentrations, very intense dye adsorption was observed. However, with the increase in dye concentrations, the sorption amounts increased slowly after which the equilibrium was achieved. This indicates the fact that the adsorption sites were saturated at high dye concentration because at the adsorbent surface there is a limited number of binding sites. At equilibrium, the adsorption capacity of methylene blue achieves 64 mg/g. Compared to other common adsorbents studied in the literature (Table 2), this registered amount of Methylene blue removal is interesting and thus the prepared copper nanoparticles from *Cynomorium coccineum* extract could be seen as a good adsorbent. As an example, this value registered for copper oxide nanoparticles is about four times higher than the sorption capacity registered within multi-wall carbon nanotubes (15.9 mg/g) (Ji-Lai et al., 2009) and hydroxyapatite nanoparticles (14.7 mg/g) (Wei et al., 2005) used as adsorbents of Methylene Blue. It is about three times higher than zeolites prepared from kaolins collected from different sources (21.4 mg/g) (El-Mekkawi et al., 2016).

Experimental results show that as the temperature was increased from 22 to 55 °C, the adsorbed quantity of dye slightly increased (Fig. 5d). At 55 °C, q_t is about 73 mg g^{-1} and it is 64 mg g^{-1}, after equilibrium at 22 °C. The improved dye removal with an increase in temperature may be attributed to the kinetic effects due to the enhanced diffusion of the dye molecules or it can be attributed to new adsorption sites being "activated" (Zhou et al., 2014) on the prepared nano-adsorbents at high temperature. This physicochemical behavior can be attributed to the possibility of enlargement of the pore sizes of the sorbent particles at high temperature. The elevated temperature can, moreover, break the internal bonds near the edge of the active sites thus increasing the sorption capacities (Weng et al., 2009). According to Güzel et al. (2015), these trends may be clarified by the fact that the increase in temperature adds strength to the adsorbate molecule scatter rate across the external limit layer and the internal pores of the adsorbent particles as a result of reduced solution's viscosity.

3.3. Kinetic study

The adsorption rate was checked using four kinetic models: pseudo-first order, pseudo-second-order, Elovich, and Intra-particular Diffusion to understand the possible mechanisms involved in the adsorption process of methylene blue in the
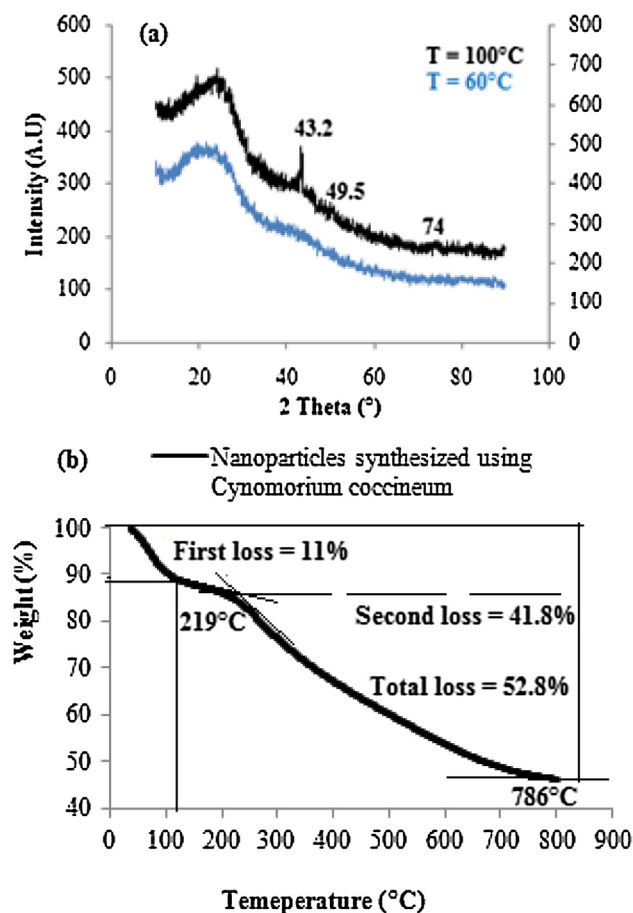
Fig. 5 (a) XRD patterns, and (b) TGA curves of the synthesized copper nanoparticles using *cynomoriumcoccineum* extract.
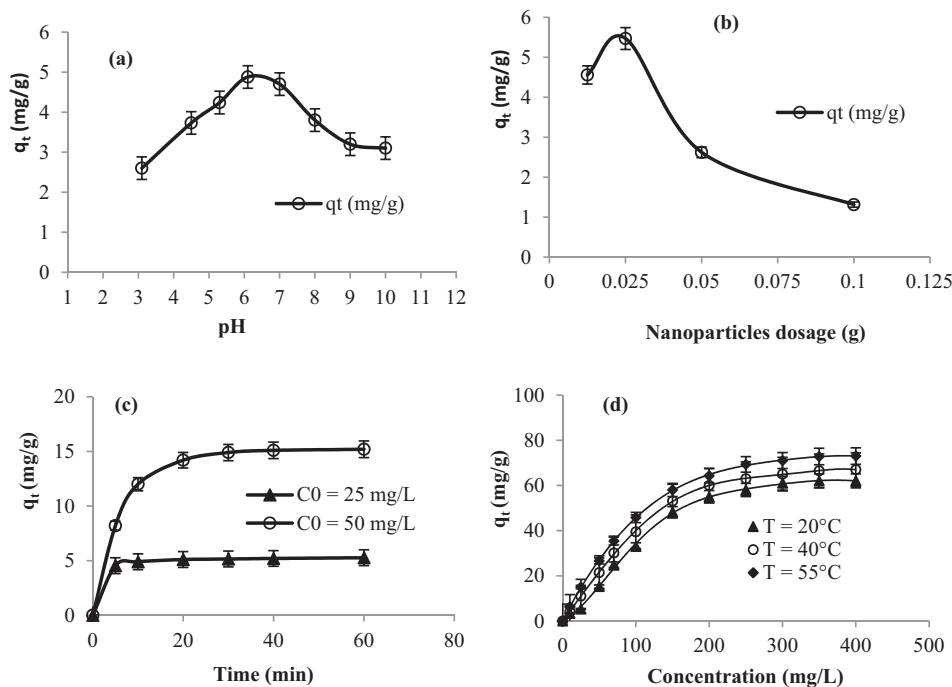
presence of the synthesized nano-adsorbents. The fitting curves and the computed kinetic parameters were presented in Fig. 6 and Table 3, respectively. The conformity between experimental data and the model predicted values was expressed by the correlation coefficients R^2 and the comparison of calculated with experimental adsorption capacities. The pseudo-first-order model (Fig. 7a) yielded relatively low R^2 values (0.89–0.92). Hence it could not describe the kinetic data in this case. It is reported that the pseudo-first-order equation does not fit well with the whole range of contact time in the adsorption experiments and it remains generally applicable over the initial stage of the adsorption processes (Mazengarb and Roberts, 2009). However, following the pseudo-second-order data (Fig. 7b), excellent linearity was observed. The correlation coefficients are greater than 0.99 associated with the decrease of the rate constant k2 with increasing initial dye concentration. Moreover, the registered experimental sorption capacities are close to those calculated theoretically. These trends suggest that the chemi-sorption was so significant (Gucek et al., 2005). Regarding the intraparticle diffusion data (Fig. 7d), the plots were deviated from the origin indicating that this equation was not the sole rate-controlling step but more than one kinetic process was involved in the adsorption process (Ho and McKay, 1998).

3.4. Isotherms study and thermodynamic parameters determination

The study of the adsorption isotherms remains a useful strategy to describe both the relationship between the adsorbate concentration in the solution and the solid adsorbent at a constant temperature and the design adsorption systems. In this study, Langmuir, Freundlich, Temkin, and Dubinin–

Fig. 6 Effect of: (a) pH value (C_0 = 25 mg/L, T = 22 °C, time = 30 min), (b) adsorbent dosage (dye volume = 20 mL, pH = 6, C_0 = 25 mg/L, T = 22 °C), (c) time contact, and (d) dye concentration on the adsorption capacity in the presence of the synthesized nano-adsorbents.

Table 2 Comparison of the adsorption capacities of methylene blue using various adsorbents studied in the literature.

Adsorbents	q_{max} (mg g^{-1})	References
Nano-adsorbents prepared from *Cynomorium coccineum* extract	64	Current study
magnetic multi-wall carbon nanotube nanocomposite	15.9	Ji-Lai et al. (2009)
crystalline hydroxyapatite nanoparticles	14.7	Wei et al. (2005)
zeolites prepared from Egyptian kaolins	21.4	El-Mekkawi et al. (2016)
Titane nanotubes	133.3	Xiong et al. (2010)
Cu@ Mn-ZnS-NPs-AC	72.90	Dastkhoon et al. (2017)
ZnO: Au-NR-AC	107.5	Bazrafshan et al. (2017)
Zn(OH)2-NPs-AC from Cherry Tree	41.49	Bazrafshan et al. (2017)
Gelatine-12.5%Bentonite	70.97	Li et al. (2018)

Table 3 Summarized kinetic constants, Langmuir, Freundlich, Temkin and Dubinin-Radushkevich parameters for the adsorption of methylene blue using nano-adsorbents synthesized from *Cynomorium coccineum* extract.

Kinetic data				Isotherms data				
Kinetic equations	Constants	Dye concentration (mg/L)		Isotherms	Parameters	Temperature values (°C)		
Pseudo First order		25	50			22	40	55
	K_1 (min^{-1})	0.034	0.035	Langmuir	q_L (mg g^{-1})	125	111.11	111.11
	q_e (mg g^{-1})	1.63	8.41		K_L (L g^{-1})	0.0032	0.005	0.007
	R^2	0.89	0.92		R^2	0.87	0.95	0.98
Pseudo-second Order	K_2	0.066	0.004	Thermodynamic	$\Delta H°$ (kJ mol^{-1})	19.07		
	q_e	5.35	16.39	parameters	$\Delta S°$ (J mol^{-1})	16.91		
	h	4.69	1.08		$\Delta G°$ (kJ mol^{-1})	14.08	13.78	13.52
	R^2	1	0.99	Freundlich	K_F (L g^{-1})	2.08	1.021	1.82
Elovich	α	849,187	15.42		n	1.16	1.34	1.52
	β	3.57	0.36		R^2	0.95	0.95	0.95
	R^2	0.93	0.89	Temkin	B (J/mol)	19.23	19.65	20.55
Intra-particular- diffusion	K_{id} (mg g^1 min$^{1/2}$)	0.57	1.94		A(L g^{-1})	0.069	0.084	0.098
					b_t (J/mol)	127.54	132.43	132.7
	R^2	0.61	0.82		R^2	0.94	0.97	0.97
				Dubinin-Radushkevich	q_{DR} (mg g^{-1})	38.09	45.56	51.62
					K_{DR} (mol^2/kJ^2)	5×10^{-5}	4×10^{-5}	3×10^{-5}
					E (KJ/mol)	100	111.8	129.1
					R^2	0.61	0.73	0.73

q_e (mg/g) is the capacity of adsorption at equilibrium, k_1 (1/min) is the pseudo-first-order rate constant.
k_2 is the rate constant for pseudo-second-order adsorption (g/mg/min), h (mg/g/min) is the initial adsorption rate.
q_L is the maximum adsorption capacity (mg/g) for a complete monolayer coverage, K_L is the Langmuir isotherm constant (L/g).
α (mg/g/min) is the constant considered as the initial sorption rate and β(mg/g) is the desorption constant during any one experiment.
k_{id} is the intra-particle diffusion rate constant (mg/g/min).
K_F and n are the Freundlich constants, describing the adsorption capacity and intensity, respectively.
b_t is the Temkin constant related to the heat of adsorption (J/mol), B is Temkin constant related to maximum binding energy (J/mol) and A is the equilibrium binding constant (L/mg).
q_{DR} (mg/g) is the adsorption capacity, K_{DR} (mol^2/kJ^2) is a constant related to the sorption energy, E is the mean free energy of adsorption for each molecule of the adsorbate.

Radushkevich models (Fig. 8) were employed to describe the adsorptive behavior of methylene blue in the presence of the prepared nanoadsorbents. The fitting parameters using the four studied models are summarized in Table 3. The isotherm model's validity was confirmed by comparing the R^2 values. The assessment of the results shows that Temkin isotherm fitted better to methylene blue adsorption data (0.94 < R^2 < 0.97) compared to the three other models. The values of B and b_t, calculated using Fig. 8c, increased with increase in temperature (22–50 °C), indicating endothermic adsorption and strong dye-nano-adsorbent interaction (Equbal Ahmad Khan, 2018). The Temkin isotherm assumes that the bonding energy of adsorption decreases linearly with increasing surface coverage (Temkin and Pyzhev, 1940). Whereas, the Dubinin Radushkevich isotherm is generally applied to express the adsorption mechanism with a Gaussian energy distribution onto a heterogeneous surface (Dubinin, 1960). From the calculated parameters of the Dubinin Radushkevich model, provided in Table 3, the mean free energy (E) was found to be 100–129.1 kJ/mol indicating a chemi-sorption process of methylene blue onto a heterogenous surface. If there are any adsorbate-adsorbate interactions, they are best described by the Temkin isotherm. Herein, the Temkin isotherm plots for methylene blue adsorption in the presence of
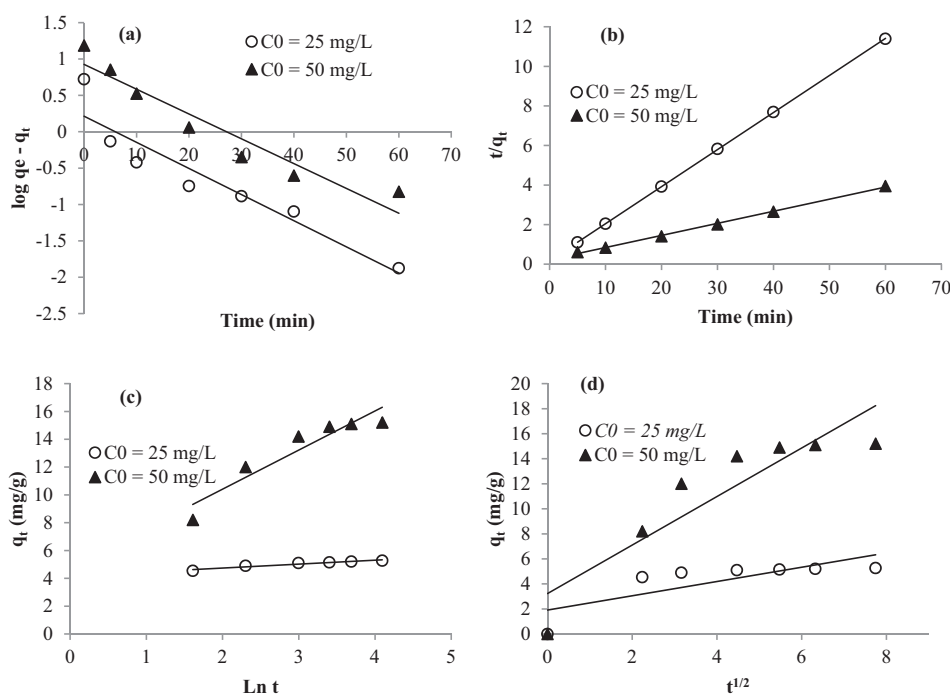
Fig. 7 Linearization of the kinetic data through: (a) Pseudo First Order, (b) Pseudo Second order, (c) Elovich, and (d) Intra-particle Diffusion.

the prepared nanoparticles was linear with an R^2 of a range 0.94–0.97 demonstrating that adsorbate-adsorbate and adsorbate-nano-adsorbent interactions both control the dye removal process. Additionally, the parameters of the Temkin model, summarized in Table 3 show higher values of the heat of sorption (b_t = 127.54–132.7 J/mol) suggesting chemical adsorption for methylene blue sorption. The same trends were also observed within the work of Ngulube et al. (2018) when developing calcined magnesite as adsorbents for cationic and anionic dyes.

The favorability of the adsorption of methylene blue using the prepared nanoadsorbents could be assessed through the exponent "n" determined from Freundlich parameters and it has observed that n ranges from 1.16 to 1.52. It was reported that when the value of n lies between 1 and 10 it represents beneficial adsorption (Aljeboree et al., 2017).

The enthalpy ($\Delta H°$) and the entropy ($\Delta S°$) values were determined from plotting Ln (K_L) as a function of the inverse of the temperature (1/T) (Fig. 7e). The positive value of the enthalpy ($\Delta H°$ = 19.07 kJ/mol) confirms that the interaction between the prepared nano-adsorbent and methylene blue is endothermic. This result is also supported by the increase of the capacity removal with temperatures values, as described above. The positive value of the entropy change ($\Delta S°$ = 16.91 J/mol) displays the increased disorder and randomness at the solid-solution interface of methylene blue with the nano-adsorbents that brings about some structural changes in the dye as adsorbate and the nanoparticles as adsorbent (Elmorsi, 2011). Indeed, it was reported that this trend could reflect the affinity of the prepared nano-adsorbent towards dye molecules (Barkat et al., 2009). The positive values of the free energy ($\Delta G°$ = 13.52–14.08 kJ/mol) means that the sorption of methylene blue is non spontaneous.

4. Conclusion

Herein, nano-adsorbents were successfully prepared for the first time using *Cynomorium coccineum* extract, in which the biological extract acts as a capping as well as a reducing agent. Evidence of the formation of the metal nanoparticles was confirmed structurally and morphologically using FT-IR, SEM, XRD, EDX, and TGA. FT-IR has shown the presence of the functional groups characteristics of the studied biological extract. The purity of the particles was confirmed through EDX, showing the presence of elemental copper oxide which was surrounded with some elements of the plant. The crystalline nature of the particles was found to be affected by the temperature of drying. The average crystallite size was calculated to be about 14.2 nm. The results registered within the TGA analysis was in agreement within those reported using EDX. The prepared nanoparticles exhibited outstanding performance in the adsorption of cationic dyes. The bio-sorption capacity achieved 64 mg/g at room temperature which is a level compared to some other adsorbents previously published in the literature. The values of B and b_t indicated endothermic adsorption and strong dye-nanoadsorbent interaction. The mean free energy (E = 100–129.1 kJ/mol), calculated from Dubinin-Radushkevich suggested a chemi-sorption phenomenon. Considering the environmentally friendly plant support and the good sorption performances, the prepared nanoparticles could be used for the purification of contaminated waters and explored in other environmental applications. Further works will be extended for the development of new metallic nanoparticles using other biological extracts and it will be interesting to check their performances in photocatalysis and textile printing.
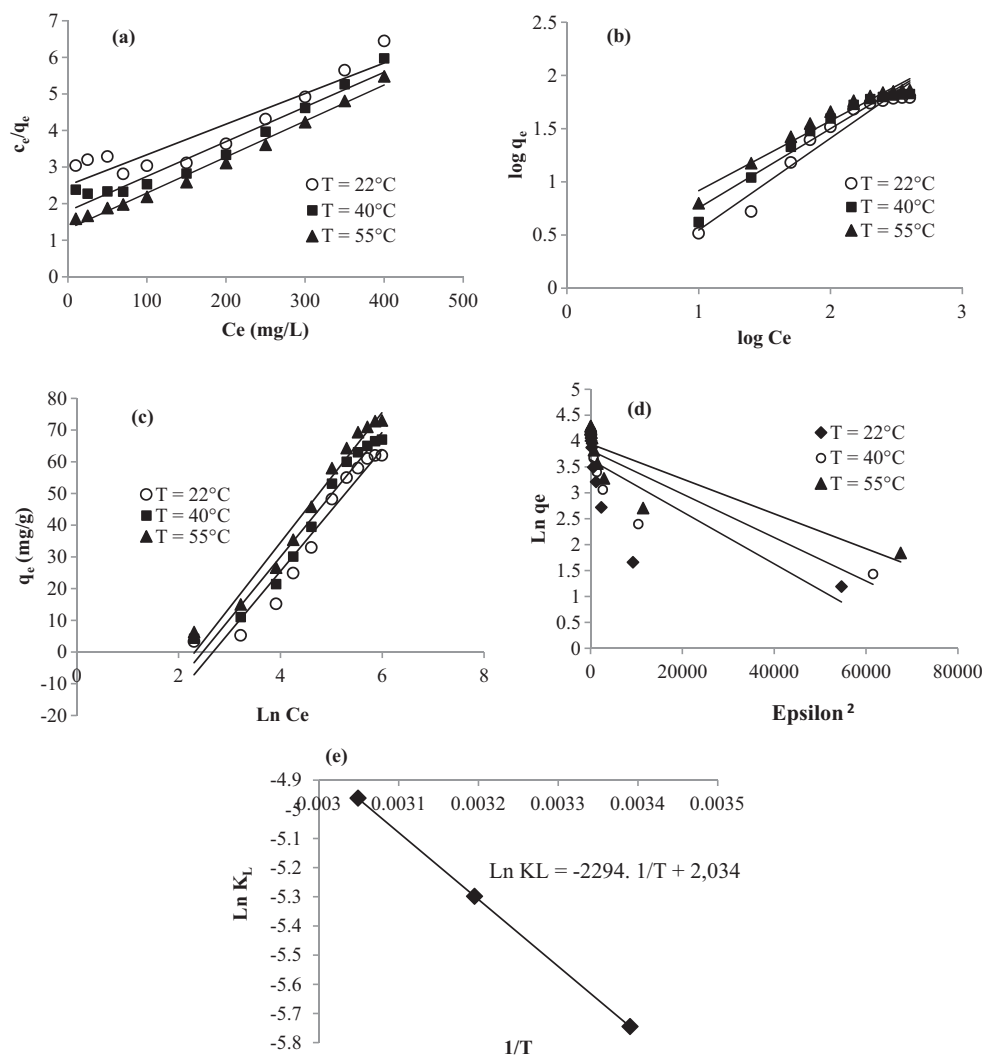
Fig. 8 Experimental data modeled using (a) Langmuir, (b) Freundlich, (c) Temkin, (d) Dubinin-Radushkevich equations, and (e) plots of Ln K_L versus the inverse of temperature.

Declaration of Competing Interest

The Author declares no conflict of interest.

References

Abd El-Rahman, H.A., El-Badry, A.A., Mahmoud, O.M., Harraz, F. A., 1999. The effect of the aqueous extract of Cynomorium coccineum on the epididymal sperm pattern of the rat. Phytother. Res. 13, 248–250.

Ahmad Khan, Equbal, Shahjahan, Alam Khan, Tabrez, 2018. Synthesis of magnetic iron-manganese oxide coated graphene oxide and its application for adsorptive removal of basic dyes from aqueous solution. Environ. Proc. Sust. Energy, 1–16.

Aljeboree, A.M., Abbas, N., Alshirifi, A.N., Alkaim, A.F., 2017. Kinetics and equilibrium study for the adsorption of textile dyes on coconut shell activated carbon. Arab. J. Chem. 10, 3381–3393.

Angrasan, J.K.V.M., Subbaiya, R., 2014. Biosynthesis of copper nanoparticles by Vitis vinifera leaf aqueous extract and its antibacterial activity. Int. J. Curr. Microbiol. App. Sci. 3, 768–774.

Aromal, S.A., Philip, D., 2012. Green synthesis of gold nanoparticles using Trigonella foenumgraecum and its size-dependent catalytic activity. Spectrochim. Acta Part A: Mol. Biomol. Spect 97, 1–5.

Barka, N., Abdennouri, M., Makhfouk, M.E.L., 2011. Removal of Methylene Blue and Eriochrome Black T from aqueous solutions by adsorption on Scolymus hispanicus L.: kinetics, equilibrium and thermodynamics. J. Taiwan Inst. Chem. Eng. 42, 320–326.

Barkat, M., Nibou, D., Chearouche, S., Mellah, A., 2009. Kinetics and thermodynamics studies of chromium(VI) ions adsorption onto activated carbon from aqueous solutions. Chem. Eng. Process. 48, 38–47.

Bazrafshan, A.A., Ghaedi, M., Hajati, S., Naghiha, R., Asfaram, A., 2017. Synthesis of ZnO-nanorod-based materials for antibacterial, antifungal activities, DNA cleavage and efficient ultrasound-assisted dyes adsorption. Ecotoxicol. Environ. Saf. 142, 330–337.

Bulut, Y., Aydın, H., 2006. A kinetics and thermodynamics study of methylene blue adsorption on wheat shells. Desalination 194, 259–267.

Cerchier, P., Dabalà, M., Brunelli, K., 2017. Green synthesis of copper nanoparticles with ultrasound assistance. Green Process. Synth. 6, 311–316.

Dastkhoon, M., Ghaedi, M., Asfaram, A., Goudarzi, A., Mohammadi, S., Wang, S., 2017. Improved adsorption performance of nanostructured composite by ultrasonic wave: optimization through response surface methodology, isotherm and kinetic studies. Ultrason. Sonochem. 37, 94–105.

Dharmananda, S., 2011. Cynomorium. Parasitic Plant Widely Used Tradition. Med. 76, 1245–1249.

Dubinin, M.M., 1960. The potential theory of adsorption of gases and vapors for adsorbents with energetically non-uniform surface. Chem. Rev. 60, 235–266.

Duke, J.A., Duke, P.-A.K., du Cellier, J.L., 2008. Duke's Handbook of Medicinal Plants of the Bible, CRC Press Taylor and Francis Group: Boca Raton, FL, USA 552.

Ebrahimi, K., Shiravand, S., Mahmouvand, H., 2017. Biosynthesis of copper nanoparticles using aqueous extract of Capparis spinosa fruit and investigation of its antibacterial activity. M. Pharma. J. 21, 866–871.

El-Mekkawi, D.M., Ibrahim, F.A., Selim, M.M., 2016. Removal of methylene blue from water using zeolites prepared from Egyptian kaolins collected from different sources. J. Environ. Chem. Eng 4, 1417–1422.

Elmorsi, T.M., 2011. Equilibrium isotherms and kinetic studies of removal of methylene blue dye by adsorption onto Miswak leaves as a natural adsorbent. J. Environ. Protect. 2, 817–827.

Govindasamy, R., Muthu, T., Govindarasu, M., Thandapani, G., Ill-Min, C., 2018. Green approach for synthesis of zinc oxide nanoparticles from Andrographis paniculata leaf extract and evaluation of their antioxidant, anti-diabetic, and anti-inflammatory activities. Bioprocess Biosyst. Eng. 41, 1–30.

Gucek, A., Sener, S., Bilgen, S., Mazmanci, A., 2005. Adsorption and kinetic studies of cationic and anionic dyes on pyrophyllite from aqueous solutions. J. Coll. Interf. Sci. 286, 53–60.

Güzel, F., Sayğılı, H., Sayğılı, G.A., Koyuncu, F., 2015. New low-cost nanoporous carbonaceous adsorbent developed from carob (Ceratonia siliqua) processing industry waste for the adsorption of anionic textile dye: characterization, equilibrium and kinetic modeling. J. Mol. Liq. 206, 244–255.

Hao-Cong, M., Shuo, W., Ying, L., Yuan-Yuan, K., Chao-Mei, M., 2013. Chemical constituents and pharmacologic actions of *Cynomorium* plants. Chin. J. Nat. Med. 11, 321–329.

Harne, S., Sharma, A., Dhaygude, M., Joglekar, S., Kodam, K., Hudlikar, M., 2012. Novel route for rapid biosynthesis of copper nanoparticles using aqueous extract of Calotropis procera L. latex and their cytotoxicity on tumor cells. Colloids Surf. B: Biointerfaces 95, 284–288.

Heestra, H., Al-Hassan, H., Minwer, F., 1990. Plants of the Northern Saudi Arabia, An Illustrated Guide. Range and Animal Development Centre Publications, Skaka, Saudi Arabia, pp. 170–171.

Ho, Y.S., McKay, G., 1998. The kinetics of sorption of basic dyes from aqueous solution by sphagnum moss peat. Can. J. Chem. Eng. 76, 822–827.

Hou, C., Wang, J., Du, W., Wang, J., Du, Y., Liu, C., Zhang, J., Hou, H., Dang, F., Zhao, L., Guo, Z., 2019. One-pot synthesized molybdenum dioxide-molybdenum carbide heterostructures coupled with 3D Holey carbon nanosheets for highly efficient and ultrastable cycling lithium-ion storage. J. Mater. Chem A 7, 13460–13472.

Ikram, M., Dar, M.S., Fakouhi, T., 1978. Hypotensive agent from *Cynomorium coccineum*. Pahlavi Med. J. 9, 167–181.

Jabli, M., 2017. Extraction of eco-friendly natural dyes from Tradescantia pallida Purpurea and Cynomorium coccineum growing naturally in Tunisia. Trends Text. Eng. Fashion Technol. 1, 1–4.

Ji-Lai, G., Wang, B., Guang-Ming, Z., Chun-Ping, Y., Cheng-Gang, N., Qiu-Ya, N., Wen-Jin, Z., Liang, Y., 2009. Removal of cationic dyes from aqueous solution using magnetic multi-wall carbon nanotube nanocomposite as adsorbent. J. Hazard. Mater. 164, 1517–1522.

Kasthuri, J., Kathiravan, K., Rajendiran, N., 2009. Phyllanthin-assisted biosynthesis of silver and gold nanoparticles: a novel biological approach. J. Nanopart. Res. 11, 1075–1085.

Li, C., Iqbal, M., Jiang, B., Wang, Z., Kim, J., Nanjundan, A.K., Whitten, A.E., Yamauchi, K.W.Y., 2019. Pore-tuning to boost the electrocatalytic activity of polymeric micelle-templated mesoporous Pd nanoparticles. Chem. Sci. 10, 4054–4061.

Li, W., Ma, Q., Bai, Y., Xu, D., Min, W., Ma, H., 2018. Facile fabrication of gelatin/bentonite composite beads for tunable removal of anionic and cationic dye. Chem. Eng. Res. Des. 134, 336–346.

Ma, L., Li, N., Wu, G., Song, G., Li, X., Han, P., Wang, G., Huang, Y., 2018. Interfacial enhancement of carbon fiber composites by growing TiO_2 nanowires onto amine-based functionalized carbon fiber surface in supercritical water. Appl. Surf. Sci. 433, 560–567.

Mazengarb, S., Roberts, G.A.F., 2009. Studies on the diffusion of direct dyes in chitosan film. Prog. Chem. App. Chitin Derivat. 14, 25–32.

Mukunthan, K., Balaji, S., 2012. Cashew apple juice (Anacardium occidentale L.) speeds up the synthesis of silver nanoparticles. Int. J. Green Nanotechnol. 4, 71–79.

Nagar, N., Devra, V., 2018. Green synthesis and characterization of copper nanoparticles using *Azadirachtaindica* leaves. Mat. Chem. Phys. 213, 44–51.

Ngulube, T., Gumbo, J.R., Masindi, V., Maity, A., 2018. Calcined magnesite as an adsorbent for cationic and anionic dyes: characterization, adsorption parameters, isotherms and kinetics study. Heliyon 4, 838.

Osasona, I., Faboya, O.L., Oso, A.O., 2013. Kinetic, equilibrium and thermodynamic studies of the adsorption of methylene blue from synthetic wastewater using cow hooves. Br. J. Appl. Sci. Technol. 3, 1006–1021.

Patel, B.H., Channiwala, M.Z., Chaudhari, S.B., Mandot, A.A., 2016. Biosynthesis of copper nanoparticles; its characterization and efficacy against human pathogenic bacterium. J. Env. Chem. Eng. 4, 2163–2169.

Saleh, T.A., 2015a. Mercury sorption by silica/carbon nanotubes and silica/activated carbon: A comparison study. Journal of Water Supply: Research and Technology - AQUA 64 (8), 892–903.

Saleh, T.A., 2015b. Isotherm, kinetic, and thermodynamic studies on Hg(II) adsorption from aqueous solution by silica- multiwall carbon nanotubes. Environmental Science and Pollution Research 22 (21), 16721–16731.

Saleh, T.A., 2016. Nanocomposite of carbon nanotubes/silica nanoparticles and their use for adsorption of Pb(II): from surface properties to sorption mechanism. Desalination and Water Treatment 57 (23), 10730–10744.

Saleh, T.A., Al-Absi, A.A., 2017. Kinetics, isotherms and thermodynamic evaluation of amine functionalized magnetic carbon for methyl red removal from aqueous solutions. Journal of Molecular Liquids 248, 577–585.

Saleh, T.A., 2018. Simultaneous adsorptive desulfurization of diesel fuel over bimetallic nanoparticles loaded on activated carbon. Journal of Cleaner Production 172, 2123–2132.

Saranyaadevi, K., Subha, V., Ravindran, R.S.E., Renganathan, S., 2014. Synthesis and characterization of copper nanoparticle using Capparis Zeylanica leaf extract. Int. J. Chem. Tech. Res. 6, 4533–4541.

Sebeia, N., Jabli, M., Ghith, A., Elghoul, Y., Alminderej, F.M., 2019. Populus tremula, nerium oleander and pergularia tomentosa as sources of cellulose and lignin for the bio-sorption of methylene blue. Int. J. Biol. Macromol. 121, 655–665.

Shankar, S.S., Rai, A., Ahmad, A., Sastry, M., 2004. Rapid synthesis of Au, Ag, and bimetallicAu core–Ag shell nanoparticles using

Neem (Azadirachta indica) leaf broth. J. Colloid Interface Sci. 275 (2), 496–502.

Sheikholeslami, M., Mahian, O., 2019. Enhancement of PCM solidification using inorganic nanoparticles and an external magnetic field with application in energy storage systems. J. Clean. Prod. 215, 963–977.

Shi, Z., Xu, G., Deng, J., Dong, M., Murugadoss, V., Liu, C., Shao, Q., Wu, S., Guo, Z., 2019. Structural characterization of lignin from D. sinicus by FTIR and NMR techniques. Green Chem. Lett. Rev. 12, 235–243.

Singh, R., Wagh, P., Wadhwani, S., Gaidhani, S., Kumbhar, A., Bellare, J., Chopade, B.A., 2013. Synthesis, optimization, and characterization of silver nanoparticles from Acinetobacter calcoaceticus and their enhanced antibacterial activity when combined with antibiotics. Int. J. Nanomed. 8, 4277–4290.

Subbaiya, R., Shiyamala, M., Revathi, K., Pushpalatha, R., Selvam, M.M., 2014. Biological synthesis of silver nanoparticles from Nerium oleander and its antibacterial and antioxidant property. Int. J. Curr. Microbiol. App. Sci. 3, 83–87.

Sun, H., Yang, Z., Pu, Y., Dou, W., Wang, C., Wang, W., Hao, X., Chen, S., Shao, Q., Dong, M., Wu, S., Ding, T., Guo, Z., 2019. Zinc oxide/vanadium pentoxide heterostructures with enhanced day-night antibacterial activities. J. Colloid Interf. Sci. 547, 40–49.

Suwalsky, M., Vargas, P., Avello, M., Villena, F., Sotomayor, C.P., 2008. Human erythrocytes are affected in vitro by flavonoids of Aristotelia chilensis (Maqui) leaves. Int. J. Pharm. 363, 85–90.

Tahir, K., Nazir, S., Li, B., Ullah Khan, A., HaqKhan, Z.U., Yu, P., Gong, S., UllahKhan, S., Ahmad, A., 2015. *Nerium oleander* leaves extract mediated synthesis of gold nanoparticles and its antioxidant activity. Mat. Let. 156, 198–201.

Temkin, M.I., Pyzhev, V., 1940. Kinetic of ammonia synthesis on promoted iron catalyst. Acta Physiochim. 12, 327–356.

Valodkar, M., Jadeja, R.N., Thounaojam, M.C., Devkar, R.V., Thakore, S., 2011. Biocompatible synthesis of peptide capped copper nanoparticles and their biological effect on tumor cells. Mater. Chem. Phys. 128, 83–89.

Wei, W., Yang, L., Zhong, W.H., Li, S.Y., Cui, J., Wei, Z.G., 2005. Fast removal of methylene blue from aqueous solution by adsorption onto poorly crystalline hydroxyapatite nanoparticles. Dig. J. Nanomater. Biostruct. 10, 1343–1363.

Weng, C.H., Lin, Y.T., Tzeng, T.W., 2009. Removal of methylene blue from aqueous solution by adsorption onto pineapple leaf powder. J. Hazard. Mater. 170, 417–424.

Xiong, L., Yang, Y., Mai, J.X., Sun, W.L., Zhang, C.Y., Wei, D.P., Ni, J.R., 2010. Adsorption behavior of methylene blue onto titanate nanotubes. Chem. Eng. J. 156, 313–320.

Xu, G., Shi, Z., Zhao, Y., Deng, J., Dong, M., Liu, C., Murugadoss, V., Mai, X., Guo, Z., 2019. Structural characterization of lignin and its carbohydrate complexes isolated from bamboo (Dendrocalamussinicus). Int. J. Biol. Macromol. 126, 376–384.

Yallappa, S., Manjanna, J., Sindhe, M.A., Satyanarayan, N.D., Pramod, S.N., Nagaraja, K., 2013. Microwave assisted rapid synthesis and biological evaluation of stable copper nanoparticles using T. arjuna bark extract. Spectrochim. Acta Part A: Mol. Biomol. Spect 110, 108–115.

Yuvakkumar, R., Nathanael, J., Honga, S.I., 2014. Rambutan (Nephelium lappaceum L.)peel extract assisted biomimetic synthesis of nickel oxide nanocrystals. Mater. Lett. 128, 170–174.

Zhou, K., Zhang, Q., Wang, B., Liu, J., Wen, P., Gui, Z., Hu, Y., 2014. The integrated utilization of typical clays in removal of organic dyes and polymer nanocomposites. J. Clean. Prod. 81, 281–289.